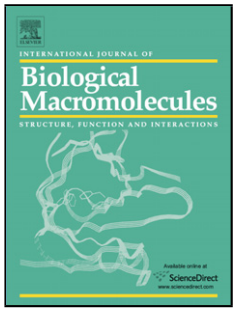

Title: Biological evaluation of p-toluene sulphonylhydrazone as carbonic anhydrase IX inhibitors: an approach to fight hypoxia-induced tumors

Authors: Aarfa Queen, Parvez Khan, Danish Idrees, Amir Azam, Md. Imtaiyaz Hassan

PII: S0141-8130(17)32590-4
DOI: http://dx.doi.org/10.1016/j.ijbiomac.2017.08.082
Reference: BIOMAC 8074

To appear in: *International Journal of Biological Macromolecules*

Received date: 17-7-2017
Revised date: 10-8-2017
Accepted date: 13-8-2017

Please cite this article as: Aarfa Queen, Parvez Khan, Danish Idrees, Amir Azam, Md.Imtaiyaz Hassan, Biological evaluation of p-toluene sulphonylhydrazone as carbonic anhydrase IX inhibitors: an approach to fight hypoxia-induced tumors, International Journal of Biological Macromoleculeshttp://dx.doi.org/10.1016/j.ijbiomac.2017.08.082

Biological evaluation of p-toluene sulphonylhydrazone as carbonic anhydrase IX inhibitors: an approach to fight hypoxia-induced tumors

Aarfa Queen[1], Parvez Khan[2], Danish Idrees[2], Amir Azam[1,*] and Md. Imtaiyaz Hassan[2,*]

[1]*Department of Chemistry, Jamia Millia Islamia, New Delhi-110025, India*
[2]*Centre for Interdisciplinary Research in Basic Sciences, Jamia Millia Islamia, New Delhi-110025, India*

Running head: CAIX Inhibitors

To whom correspondence should be addressed

Dr. Md. Imtaiyaz Hassan
Centre for Interdisciplinary Research in Basic Sciences,
Jamia Millia Islamia, New Delhi-110025, India
Tel.: +91-9990323217
E-mail: mihassan@jmi.ac.in

Prof. Amir Azam
Department of Chemistry
Jamia Millia Islamia, New Delhi-110025, India
Tel.: +91-11-26981717/3254; fax: 91-11-26980229;
E-mail: amir_sumbul@yahoo.co.in

Highlights

- Three *p*-Toluene sulphonylhydrazone derivatives are synthesized and tested for CAIX inhibition assay.
- Compound 1 and 2 bind CAIX with high affinity.
- Both compound 1 and 2 inhibits CAIX enzyme activity with IC_{50} values in nM range.
- These compounds induce apoptosis in hypoxic HeLa and HT-29 cells.

ABSTRACT

To find potential inhibitors of human carbonic anhydrase IX (CAIX), we have successfully deigned, synthesized and characterized three *p*-Toluene sulphonylhydrazone derivatives (**1-3**). Molecular docking studies provided the structural basis of CAIX inhibition and a deeper insight into the protein-ligand interactions. *p*-Toluene sulphonylhydrazone derivatives show a well organized conformational compatibility with the active site of CAIX. This protein-ligand complex was stabilized by several non-covalent interactions offered by residues present in the active site cavity. The actual binding affinity of synthesized compounds with CAIX was experimentally measured by fluorescence and isothermal titration calorimetry (ITC). Results of both fluorescence binding and ITC measurements show the binding affinity of *p*-Toluene sulphonylhydrazone derivatives to the CAIX in the μM range. CAIX enzyme inhibition assay showed the IC_{50} values in nM range. Though all the three compounds (**1-3**) showed a good binding with CAIX, compound **2** showed the best inhibition of CAIX activity. These compounds were non-toxic on normal cell lines (HEK-293) and significantly inhibit the proliferation of hypoxic cancer cells. All compounds induce apoptosis in the hypoxic cancer cells. These compounds may be further exploited as promising therapeutic agents to control the hypoxia-induced tumors.

Keywords: CAIX Inhibitors; Tumor Hypoxia; Enzyme inhibition

1. Introduction

Cancer is one of the leading causes of human death. A large number of drug therapies have been employed to fight cancer but still an effective medication is required [1, 2]. In last few decades, some potential drug targets of human cancer have been identified which

includes carbonic anhydrase (CA) [3-7], an enzyme involved in the pH regulation. CA is a zinc containing metallo-protein that efficiently catalyze the reversible hydration of carbon dioxide [6]. Among the 14 isoforms of CA, CAIX is a transmembrane isoform having extracellular-facing catalytic site [6, 8]. CAIX is known to possess highest H^+ transfer rate among all the isoforms [9].

CAIX is up-regulated in several cancers and plays significant role in tumor acidification (tumor hypoxia), progression and metastasis [9, 10]. Hypoxia conditions upregulates the expression of CAIX and therefore, its expression measure of hypoxia. High expression of CAIX generally correlates with poor prognosis. Hence, it is an important prognostic indicator in oncology [11, 12]. CAIX is present in around tumor which regulates pH by ion transport across the plasma membrane and thus guard tumor cells from acidosis, thereby balancing the intracellular accumulation of acidic metabolic products [9, 13]. The use of CAIX expression is an attractive and promising candidate marker for systemic anticancer therapy [10, 14, 15].

The detection and characterization of hypoxic areas in the solid tumor is an important topic of discussion in cancer research since hypoxia itself is an independent predictor of death in various types of cancer [14]. Hypoxic cancerous cells do not respond to chemotherapies and radiation therapies [2, 14, 16]. Thus, an approach for molecular imaging based on synthesis of selective ligands or inhibitors of CAIX which is overexpressed at sites of hypoxia is required. Such an approach could help to design and target selective potent inhibitors of CAIX for clinical uses to fight against cancer and act as anti-hypoxia therapy [15].

Sulfonamides, sulfamates, sulfamides, phenols and coumarins are some of the carbonic anhydrase inhibitors [17-20]. Sulphonamide causes the inhibition of catalytic activity of CA, by regulating acid-base balance and transport of ion in many tissues. CAIX sulphonamide

inhibitors gets accumulated in hypoxic cells only and thereby causing the reversal of acidification by CAIX [21]. Acetazolamide is a potent CA inhibitor that inhibits in the nanomolar range, ethoxolamide and topiramate are some other known CA inhibitors (**Fig. 1**) [22]. Benzene sulfonamides are classical CA inhibitors bearing various substituents, which bind to zinc ion in a deprotonated form (RSO_2NH^-) by exchanging a water molecule [23]. Recently, some other inhibitors such as thiourea derivatives [15, 24] and sulfonyl semicarbazide derivatives have been reported [25, 26] **(Fig. 1)**.

Despite a number of novel potent CA inhibitors have been synthesized, the selectivity of CA isozyme is still a mystery [27]. Hydrazone derivatives are extensively studied pharmacophore having wide range of biological activities [28, 29]. Some hydrazone derivatives of 2,6-dimethylimidazo (2,1-b) (1,3,4)thiadiazole-5-carbohydrazide [30], hydrazinopyrimidine-5-carbonitrile derivatives [31], coumarin substituted hydrazide–hydrazone derivatives [32] are known to possess anticancer activities [33] .

In view of the above properties of the sulphonamide and hydrazone skeletons, we have selected and synthesized three compounds in which the two above mentioned pharmacophore (sulphonamide and hydrazone) were covalently linked to generate a single hybrid molecule **(Fig. 2)**. Selected compounds were synthesized and evaluated against the human CAIX isozyme in anticipation that the hybrid molecules would show potent activity of the two scaffolds. The *in vitro* results of the hybrids were further validated by molecular docking, enzyme inhibition and binding studies. These compounds were further investigated for their anticancer properties and used to analyze their apoptotic potential against human cancer cell lines in normoxic as well as in hypoxic conditions.

2. Material and Methods

2.1. Materials used

N-lauryl sarcosine, MTT (3-[4,5-dimethylthiazol-2-yl]-2,5-diphenyl tetrazolium bromide) and other reagents were purchased from Sigma Aldrich (St. Louis, MO). Ni-NTA column and gel filtration column (Superdex-200) were purchased from GE healthcare (GE Healthcare Life Sciences, Uppsala, Sweden). HeLa (human cervical cancer cells), human colon carcinoma cells (HT-29), and human embryonic kidney cells (HEK-293) cells were procured from National Centre for Cell Sciences (NCCS), Pune, India. FITC-Annexin-V detection kit was purchased from BD-Pharmingen, BD Biosciences (USA). Dulbecco minimal essential medium (DMEM), RPMI-1640 and Ham's F-12 nutrients mix cell culture medium and fetal bovine serum (FBS) was purchased from Gibco life sciences. All reagents used were of molecular biology grade. All the reagents, chemicals and solvents were purchased from Sigma–Aldrich (St. Louis, MO, USA), S.D Fine Chemicals (India) and Merck (Darmstadt, Germany). The purity of the compounds was tested by thin layer chromatography (TLC).

2.2. Synthesis of inhibitors

The selected compounds were synthesized by earlier reported method [34, 35]. The synthetic pathway leading to target compounds (**1–3**) is depicted in Scheme 1 (see supplementary data). Briefly, *p*-Toluene sulfonyl chloride was stirred in excess of hydrazine hydrate until a white precipitate of p-toluene sulfonyl hydrazide was formed. *p*-Toluene sulfonyl hydrazide reacted with different derivatives of aldehydes in ethanol to get hydrazones which was crystallised to give final products. All the melting points of the synthesized compounds were determined in pyrex capillaries using a basic melting point apparatus and were not corrected. Pre-coated aluminum sheets (silica gel 60 F254, Merck Germany) were used for thin-layer chromatography (TLC) and spots were visualized under UV light. Elemental analysis was carried out on CHNS Elementar (Vario EL-III) and the

results were within ± 0.3% of the theoretical values. IR spectra were recorded on Bruker FT-IR spectrophotometer on a Zn Se crystal as KBr discs. ^{1}H NMR and ^{13}C NMR spectra were recorded on Bruker Spectrosp in DPX 400 MHz using DMSO-d_6 as a solvent and tetramethylsilane (TMS) as an internal standard. Splitting patterns are designated as follows; s, singlet; d, doublet; m, multiplet. Chemical shift values are given in ppm. The FAB mass spectra of the compounds were recorded on JEOL SX 102/DA-6000 mass spectrometer using Argon/Xenon 6KV, 10 mA) as the FAB gas and m-nitro benzyl alcohol (NBA) was used as the matrix.

2.2.1. General procedure for the synthesis of p-Toluenesulfonyl hydrazide

A slight excess of hydrazine hydrate (2 mL) was added to a stirring solution of *p*-toluene sulfonyl chloride (2 gm, 10.49 mmol) at 25°C. The reaction mixture was stirred at room temperature for overnight. Solid precipitates were filtered and washed with water, to remove hydrazine hydrochloride. White hydrazide obtained was recrystallized from ethanol to give pure product.

2.2.2. General procedure for the synthesis of p-Toluenesulfonyl hydrazones (1-3)

To a stirring solution of *p*-Toluene sulfonyl hydrazide (0.25 g, mmol) in ethanol one equivalent of different substituted aldehyde was added. The reaction mixture was stirred at room temperature for 12h to get precipitate of hydrazone which was filtered dried and recrystallized from ethanol.

2.3. Molecular docking

The atomic co-ordinate of CAIX was taken from protein data bank (www.rcsb.org, PDBID: 3IAI), and optimized using steepest descent method from Gromacs 4.5.5. The 2D

and 3D structures of all the synthesized compounds were drawn with the help of Chembio Draw ultra. Further calculations and file preparations are done according to our published protocol [15, 36]. After preparing the coordinate files of CAIX and respective compound, it was subjected to docking using AutoDock 4 package [37]. The interaction between CAIX and each compound were analyzed using the Lamarckian genetic algorithm (LGA). The binding energy was calculated using van der Waals, electrostatic interactions and hydrogen bonding. Finally docked complexes of CAIX were further optimized, validated and explored using "Receptor–Ligand Interactions" modules of Discover Studio 4.0 [38].

2.4. Expression and purification of proteins

CAIX and CAII were successfully expressed in *E. coli* (BL21 strain) and subsequently purified [15, 39, 40]. In brief, for CAIX the pellet obtained from the culture was dissolved in cell-lysis buffer (50mM Tris, 250mM NaCl, 0.1 mM PMSF and 1% Triton-100) and inclusion bodies were prepared. Further, inclusion bodies were dissolved in sarcosine buffer (50mM Tris, 1.5% N-laurosyl sarcosine, pH 8.0) and were centrifuged for 25 min at 12,000 rpm and the supernatant was collected. From this supernatant, CAIX protein was purified using Ni-NTA affinity chromatography. In case of CAII, expression vector containing gene of CAII, expressed in *E. coli* (BL21 strain). After cell lysis, filtered supernatant was loaded on Ni-NTA affinity column, pre-equilibrated with Tris-HCl buffer (pH 7.5, 500 mM NaCl and 5% Glycerol). The eluted protein was concentrated and further purified by gel-filtration chromatography (Superdex 200 pg connected to the Akta purifier, GE Healthcare). The purity of eluted CAIX and CAII was then checked by running SDS-PAGE.

2.5. Fluorescence measurements

The binding study of each synthesized compounds with that CAIX protein was carried by monitoring changes in fluorescence intensity of protein. The stock solutions of synthesized compounds were made in the DMSO, and diluted to 1 µM/µl working concentration in the 50 mM phosphate buffer. All fluorescence experiments were carried out on Jasco spectroflourimeter (FP-6200) using a 5 mm quartz cuvette (excitation at 280 nm, emission at 300-400 nm). To obtain final spectra, each time corresponding blank is subtracted. Each experiment was performed in triplicates. A decrease in fluorescence intensity with increasing concentration of compound was utilized as a measure for the calculation of binding constant (K_a), number of binding sites present in protein (n) using the modified Stern-Volmer equation:

$$\log (F_o\text{-}F)/F = \log K_a + n\log[L] \qquad (1)$$

where, F_o = fluorescence intensity of native protein, F = fluorescence intensity of protein in the presence of ligand, K_a = Binding constant, n = number of binding sites, L = concentration of ligand. The values for binding constant (K_a) and number of binding sites (n) were derived from the intercept and slope, respectively.

2.6. Isothermal titration calorimetry

Isothermal titration calorimetry (ITC) measurements were studied using a VP-ITC microcalorimeter from MicroCal, Inc (GE, MicroCal, USA) according to our published protocol [41]. Briefly, protein was extensively dialyzed against 50 mM phosphate buffer and from the stock solution of ligand working ligand solutions was prepared in last dialyzing buffer. As stock solutions of compounds was prepared in DMSO, equal amount of DMSO, according to the amount added in preparing ligand solution was added to the protein solution (up to 1.5 % v/v) in order to prevent signal stability problems during ITC measurements.

Blank experiments were carried out to obtain the heat of dilution of each compound. For analysis, heat of dilution of each compound with that of buffer was taken and subtracted from the heat of dilution obtained from the compound-protein titrations. The binding data was analysed using MicroCal Origin 7.0 software provided with the instrument.

2.7. CA inhibitory assay

CAIX and CAII enzyme inhibition assays were performed using reported method [7, 15]. This procedure is based on spectrophotometric determination of *p*-nitrophenol which is a yellow colored compound that is formed as hydrolysis product of *p*-nitrophenyl acetate (4-NPA) catalyzed by CA. The absorbance was then measured at 400nm by UV spectrophotometer V-660. The IC_{50} values for each test compounds were calculated by using Graph Pad Prism (Version 6.0) software.

2.8. Cell viability assay

The studied cell lines (HeLa and HT-29) were maximally passaged for 3 months. Cells were incubated at 37 ºC with 5 % CO_2 (for normoxic conditions), 1 % O_2 and 5 % CO_2 balanced with N2 or grown in the presence of deferoxamine (to mimic hypoxic conditions) as reported [42, 43]. We have selected HeLa and HT-29 cells because it has been reported that these cells naturally express CAIX [43]. To determine the cytotoxic and anticancerous activities of compounds, MTT assay was carried out as described [36, 41]. Briefly, 10×10^3 viable cells were seeded in a 96 well plates and incubated with increasing concentrations of compounds (5 µM-100 µM). After 48 h of treatment, mixture of medium and compound were removed, cells were washed with phosphate buffer saline (PBS) twice. Approximately, 20 µl MTT (from 5 mg/ml stock) and 100 µl DMEM was added to each well and incubated for 4-5 h at 37 ºC, in a CO_2 incubator. Finally, the residual MTT and medium was aspirated and the

crystals of formazan were dissolves by adding 100 µl DMSO in each well. The micro-titer plates were then agitated for 15-20 minutes on an orbital plate shaker and absorbance at 570 nm was taken on a titerplate reader (BioRad). Absorbance value obtained was translated into percentage viability in comparison to the control cells.

2.9. Cell apoptosis assay

To determine cell apoptosis, annexin-V staining was used [44, 45]. HeLa cells were treated with IC_{50} concentration of each compound for 24 h at 37ºC, and the control cells were treated with the media only. After 24 h, nearly $2x10^6$ cells were trypsinized and washed two times with 5-6 ml of PBS by centrifugation; at 1800 rpm for 4 min. Staining of Annexin-V was done by using FITC-Annexin-V kit by following the manufacturer's instructions (BD-Biosciences, USA). For each sample nearly, 10,000 events were taken by flow cytometry BD FACScanto and data were analyzed with help of flowJo software. DAPI was used to stain nuclei of the cells [41]. Fluorescence images were taken on Nikon-EclipseTS100 microscope.

3. Results

3.1. Synthesis

All compounds were characterized by IR, 1H NMR, ^{13}C NMR and mass spectrometry (see supplementary data). The purity of the compounds was confirmed by elemental analysis and data was found in accordance with ± 0.3 %.

3.1.1. N'-[(1E)-(2-hydroxyphenyl) methylene]-4-methylbenzenesulfonohydrazide (1)

Compound **1** was succesfully synthesized and confirmed by IR, 1H NMR, ^{13}C NMR analysis. Observations from the results of IR, 1H NMR, ^{13}C NMR are described as (White solid, Ethanol) Yield: 78 %; mp: 149-151 ^{o}C; Anal. calc. for $C_{14}H_{14}N_2O_3S$: C 57.9, H 4.9, N 9.6, O 16.5, S 11.0 %; found: C 58.1, H 4.9, N 9.5, O 16.5, S 11.2 %; IR *ν*max (cm^{-1}): 3183 (N-H), 2926 (Ar-H), 1616 (C=N), 1495 (C=C), 1330, 1168 (SO_2) ; ^{1}H NMR (DMSO-d_6) δ: 11.43(s, 1H, -NH), 10.18 (s, 1H, -OH), 8.16 (s, 1H, -CH=N), 7.75 (d, 2H, *J*=8.4 Hz, Ar-H), 7.41 (d, 2H, *J*=8.4 Hz, Ar-H), 7.23-7.19 (m, 1H, Ar-H), 6.85-6.79 (m, 2H, Ar-H), 2.34 (s, 3H-CH_3); ^{13}C NMR (DMSO- d_6) δ (ppm): 156.47, 146.19, 143.59, 135.83, 131.40, 129.72, 127.50, 127.13, 119.39, 119.00, 116.16, 20.95; ESI-MS (m/z): 291.1 (M^++1).

3.1.2. N'-[(1E)-(4-methoxyphenyl)methylene]-4-methylbenzenesulfonohydrazide (2)

Compound **2** was succesfully synthesized and confirmed by IR, 1H NMR, ^{13}C NMR analysis. Observations from the results of IR, 1H NMR, ^{13}C NMR are described as Light orange needles, 20% DCM: Hexane) Yield: 83%; mp: 102-104 ^{o}C; Anal. calc. for $C_{15}H_{16}N_2O_3S$: C 59.2, H 5.3, N 9.2, O 15.8, S 10.5 %; found: C 58.9, H 5.2, N 9.4, O 16.1, S 10.24 %; IR *ν*max (cm^{-1}): 3222 (N-H), 2842 (Ar-H), 1575 (C=N), 1520 (C=C), 1326, 1162 (SO_2); ^{1}H NMR (DMSO- d_6) δ: 11.21 (s, 1H, -NH), 7.84 (s, 1H, -CH=N), 7.75 (d, 2H, *J*=8.4Hz, Ar-H), 7.49 (d, 2H, *J*=8.8Hz, Ar-H), 7.39 (d, 1H, *J*=8.8 Hz, Ar-H), 6.93(d, *J*=8.4 Hz, 2H, Ar-H), 2.34 (s, 3H, -CH_3); ^{13}C NMR (DMSO- d_6) δ (ppm): 160.74, 147.00, 143.29, 136.19, 129.56, 128.32, 127.21, 126.25, 114.22. ESI-MS (m/z); 305.0 (M^++1).

3.1.3. N'-[(1E)-(3,4-dimethoxyphenyl)methylene]-4-methylbenzenesulfonohydrazide (3)

Compound **3** was succesfully synthesized and confirmed by IR, 1H NMR, ^{13}C NMR analysis. Observations from the results of IR, 1H NMR, ^{13}C NMR are described as (Yellow needles, 10% DCM: Hexane) Yield: 80 %; mp: 131-132 ^{o}C; Anal. calc. for $C_{16}H_{18}N_2O_4S$: C

57.5, H 5.4, N 8.4, O 19.1, S 9.6 %; found: C 57.3, H 5.2, N 8.3, O 19.2, S 9.5 %; IR *ν*max (cm^{-1}): 3198 (N-H), 2987, 2838 (Ar-H), 1583 (C=N), 1521 (C=C), 1320, 1168 (SO_2); ^{1}H NMR (DMSO- d_6) δ: 11.20 (s, 1H, -NH), 7.82 (s, 1H, -CH=N), 7.76 (s, 1H, Ar-H), 7.48 (s, 1H, Ar-H), 7.39 (s, 1H, Ar-H), 7.37 (s, 1H, Ar-H), 7.12-7.05 (m, 1H, Ar-H), 6.95 (s, 1H, Ar-H), 6.92 (s, 1H, Ar-H), 2.34 (s, 3H, $-CH_3$); ^{13}C NMR (DMSO- d_6) δ (ppm): 151.11, 149.39, 147.67, 143.82, 136.65, 130.04, 127.75, 126.92, 121.40, 112.01, 109.16:); ESI-MS (m/z): 334.9.0 (M^+ + 1).

3.2. Molecular docking

To find out the interactions between CAIX and synthesized compounds, molecular docking was carried out. Docking studies helps to estimate the binding energies, interacting residues, intermolecular distance between the atoms of ligands and interacting residues of CAIX. By following the criteria of binding energy, type and extent of interactions exists, the best-docked CAIX-ligand complexes were selected. CAIX shows a substantial binding with **1**, **2** and **3** compounds **(Table 1).** Docking suggesting that the compound **1** and **2** bind into the active site cavity of CAIX **(Fig. 3 & 4).**

All the three compounds bind with CAIX significantly **(Fig. 3 & 4).** Compound **1** forms a complex with CAIX by offering four hydrogen bonds **(Fig. 4B)**, present between Gln92, Leu198, Thr199 and Thr200 at 3.0, 3.1, 3.0 and 2.7 Å, respectively. Compound **2** forms six hydrogen bonds with His94, Thr199 (2) and Thr200 (3) residues of CAIX **(Fig. 4C)**, average distances of these hydrogen bonds are 3.3, 2.8, 3.0, 3.0, 3.0 and 2.9 Å, respectively suggesting a strong binding. Compound **3** on the other hand, offering only two hydrogen bonds, exists between Arg102 (2.2 Å) and Ser227 (3.0 Å) **(Fig. 4D)**. Analysis of docked structure shows that CAIX offers numerous van der Waals, covalent and electrostatic interactions to all the three compounds **(Fig. 3A).**

3.3 Fluorescence binding studies

To estimate the actual binding affinity of *p*-Toluene sulfonylhydrazone derivatives, fluorescence and ITC measurements were performed. Binding constants of all three compounds toward purified CAIX were determined from fluorescence-monitored compound-CAIX titration by using modified Stern-Volmer equation (equation 1). The best quenching on addition of increasing amount of compounds were observed in case of compound **1** and **2 (Fig. 5A).** For compound **3** a relatively lower intensity of quenching was observed in comparison to compound **1** and **2 (Fig. 5A).** Binding affinities of these compounds to CAIX were estimated by calculating binding constant with the help of modified Stern-Volmer plot and found Ka = 6.9×10^7 M^{-1}, Ka = 4.2×10^8 M^{-1} and Ka = 7.4×10^3 M^{-1} for compounds **1**, **2** and **3**, respectively. These results are suggesting that compound **2** is the best molecule which may be further exploited for inhibition of CAIX.

3.4. ITC measurements

To ascertain binding affinity and nature of interaction of these compounds with CAIX, we performed ITC measurement. The upper panel of **Fig. 6** displays raw data with negative heat pulsations indicating exothermic binding. After subtracting the dilutions of each compound and protein, the final ITC isotherm and fitted titration data of CAIX with each compound is shown in lower panel of **Fig. 6**. The results shown **(Fig. 6)** were obtained from single-site model of fitting. Different thermodynamic parameter associated with binding of each synthesized compound with CAIX (association constant and ΔH, enthalpy change) is shown in **Table 2**. ITC Results also confirms that although three compounds shows binding with CAIX, but binding affinity of compound **1** and **2** is relatively higher (as depicted from their dissociation constant values) and can be used as potential inhibitors against CAIX.

3.5. Enzyme inhibition assay

Enzyme inhibition potential of compounds **1**, **2**, **3** against CAIX and CAII was assayed by measuring the esterase activity of CA using nitrophenol acetate (4-NPA) as a substrate. For enzyme inhibition studies, acetazolamide was used as a positive control. We found that compounds **1**, **2** and **3** are showing appreciable inhibition of CAIX activity with an IC_{50} value of 78 nM, 56 nM and 10.89 μM, respectively. Whereas these compounds show less inhibition against CAII with following IC_{50} values, 99 μM, 90 μM and 160 μM, respectively **(Table 2).** It can be easily observed from IC_{50} values of these compounds that compound 1 and 2 inhibits CAIX more specifically than CAII.

3.6. Cell viability assay

To see the effect of synthesized compounds on the proliferation of HT-29 and HeLa cells, MTT assay was carried out. Treatment of all compounds inhibit the viability of HeLa and HT-29 cell lines in a dose-dependent (5–100 μM) manner **(Fig. 7).** IC_{50} values of each compound after 48 h treatment are given in **Table 2.** Cell viability studies on hypoxic as well as normoxic HT-29 and HeLa cells were found to be dose dependent effect of compounds (**1-3**) on the cell viabilities. Interestingly, it was found that all compounds reduce the cell viability in both conditions, but inhibition is more prominent in case of hypoxic cells as compared to normoxic cells **(Fig. 7).** It was found that compound 1 and 2 inhibits the proliferation of HT-29 and HeLa cells (both in hypoxic as well as normoxic conditions) to a greater extent than compound 3 **(Fig. 7)**.

3.7. Apoptosis assay

To further elaborate our observations regarding the functional influence of present CAIX inhibitors in terms of apoptotic potential, HeLa and HT-29 cells were treated with the

respective IC_{50} concentration of each compound for 24 h. Double staining was used to see early apoptosis (annexin-V staining) and late apoptosis (PE-staining/7-AAD). It was found that treatment of cells with compound **1**, **2** and **3** induces apoptosis in both the cancer cell lines **(Fig. 8).** Induction of apoptosis was also studied in both hypoxic as well as normoxic cells. Consistent to the cell viability studies as described in previous section, here also it was observed that though induction of apoptosis takes place in both experimental conditions (hypoxia/normoxia), but more number of cells are found to be positive for annexin-V and PE-staining when treatment is given in hypoxic conditions (see lower row of **Fig. 8A**). Another important observation from these results is that out of three studied inhibitors (**1**, **2** and **3**), if we compare efficacy, then compound **2** is most effective as it induces apoptosis in more number of cells, which was followed by **1** whereas **3** is least effective. In case of normoxic HT-29 cells compounds **1**, **2** and **3** induces apoptosis in 4.79 %, 6.49 % and 6.28 % of cells, but in hypoxic condition the percentage of apoptotic cells increases to 37.09 %, 74.1 % and 15.49 %, respectively. Similarly, compounds **1**, **2** and **3** treatment to normoxic HeLa cells prompts apoptosis in 7.86 %, 24.15 % and 7.15 % of cells, whereas in hypoxic conditions 51.39 %, 92.84 % and 19.2 % of cells found to be apoptotic, respectively. Results of DAPI-staining suggest that treatment of HeLa cells with compound **1**, **2** and **3**, induces nuclear morphological changes or nuclear fragmentation also **(Fig. 8B).** It can be easily observed from **Fig. 8B** that compound 1 and 2 induces nuclear fragmentation in more number of cells (as shown by red color open head arrows) than compound 3. It also supports the anticancerous behavior of these inhibitors effectively.

4. Discussion

Cancer is a worldwide substantial health problem. Management and prevention of cancer is necessary because of social and financial burden to the society. Despite appreciative

understanding of the diverse molecular corridors involved in progression of different types of cancer, the use of specifically targeted bio macromolecules has failed to deliver significant developments in the survival of cancer patients. Numerous reports have shown the association of various signaling pathways in the progression of different cancers [41, 46, 47]. In the field of cancer biology, now day's tumor microenvironment becomes an important hallmark that has been targeted for drug discovery [1, 48]. Uses of structural information of cancer targets to design potent inhibitors using molecular docking and simulation are extensively used to fight against different types of cancer [49-60].

CAIX becomes a prognostic indicator and important drug target. As it gets up-regulated in numerous cancers and plays a substantial role in acidification of tumor (tumor hypoxia), progression and metastasis [9, 10]. Therefore expression of CAIX is a measure of hypoxia and correlates with poor prognosis [11, 12]. High expression of CAIX is an attractive and promising candidate marker for systemic anticancer therapy and drug development [10, 14, 15, 61]. In this study we report the use of p-Toluene sulfonylhydrazone derivatives as potential inhibitors of CAIX.

Initially binding affinity of synthesized molecules with CAIX has been studied by molecular docking that suggests a relatively strong binding affinity. The compound-CAIX docked complex was stabilized by hydrogen bonding as well as π-π interactions **(Fig. 3 & 4)**. Results obtained from docking were further confirmed by the fluorescence binding and ITC measurements, showing that compound **1** & **2** binds with the CAIX with high affinity (in μM range). To further ascertain the functional significance of p-Toluene sulfonylhydrazones derivatives, enzyme inhibition assay was performed which clearly indicated a significant inhibition potential towards CAIX **(Table 2)**.

Structure analysis of compound **1** is suggesting that the hydroxy (-OH) group is more reactive and electron donating in comparison to methoxy (-OCH3) group due to steric

repulsion of the methyl group on the lone pair of oxygen. The methoxy derivative of p-toluene sulfonylhydrazone **2** possesses maximum enzyme inhibition activity against CAIX. The electron releasing methoxy group provides moderate basicity as compared to **1** which is more basic due to the presence of hydroxy group. In compound **3**, two methoxy groups lead to p-Toluene sulphonylhydrazone derivatives least basic as compared to compound **1** and **2**. Interestingly it does not bind as strongly with CAIX as compound **1** and **2**. Thus, the basicity of the compounds may influence the interaction of these compounds with CAIX. Studied compounds efficiently bind to the CAIX and appreciably inhibit the enzymatic activity of CAIX and thus they may be explored for the development of unique pharmacophore.

Cancer cells multiply in an uncontrolled fashion and are generally resilient to apoptosis in response to several chemotherapeutic drugs that has been developed in the last decades [2, 16]. Our results indicated that p-Toluene sulfonylhydrazone have the ability to sensitize hypoxic cancer cells toward apoptosis **(Fig. 8).** It is an important aspect in drug development that the synthesized drug molecule should be nontoxic or minimally toxic; our results also suggested no toxicity of synthesized molecules in the studied concentration range towards normal HEK-293 cells.

5. Conclusion

In summary, studies presented here shown that synthesized tosylhydrazine derivatives are binding to the CAIX with a significant binding affinity and resulting in inhibition of its enzyme activity which many be associated with its anticancerous activity. Further chemical modifications may be helpful to improve their binding affinity and specificity and exploited further for an effective hypoxia-induced cancer management. This study offers first evidence that p-Toluene sulfonylhydrazone derivatives bind CAIX and showed anticancer activity on different cell lines by inducing apoptosis.

Acknowledgements

This work is supported by the Council of Scientific and Industrial Research, India (grant no. 37(1665)/15/EMR-II). AQ is thankful to the University Grant Commission (UGC) India for financial support. We sincerely acknowledge Prof. Abdul Waheed, Saint Louis University for providing the gene of CAII & CAIX. Authors thank to the Department of Science and Technology, Government of India for the FIST support (FIST program No. SR/FST/LSI-541/2012).

Disclosure of Conflicts of Interest

Authors have declared that there is no any conflict of interest.

References

[1] D. Hanahan, R.A. Weinberg, Hallmarks of cancer: the next generation, Cell 144(5) (2011) 646-74.

[2] C. Holohan, S. Van Schaeybroeck, D.B. Longley, P.G. Johnston, Cancer drug resistance: an evolving paradigm, Nat Rev Cancer 13(10) (2013) 714-26.

[3] C.T. Supuran, A. Scozzafava, J. Conway, Carbonic anhydrase: its inhibitors and activators, CRC Press2004.

[4] C.T. Supuran, Carbonic anhydrases as drug targets-an overview, Current topics in medicinal chemistry 7(9) (2007) 825-833.

[5] D. Idrees, M. Shahbaaz, K. Bisetty, A. Islam, F. Ahmad, M.I. Hassan, Effect of pH on structure, function, and stability of mitochondrial carbonic anhydrase VA, J Biomol Struct Dyn 35(2) (2017) 449-461.

[6] M. Imtaiyaz Hassan, B. Shajee, A. Waheed, F. Ahmad, W.S. Sly, Structure, function and applications of carbonic anhydrase isozymes, Bioorg Med Chem 21(6) (2013) 1570-82.

[7] S. Kumari, C.B. Mishra, D. Idrees, A. Prakash, R. Yadav, M.I. Hassan, M. Tiwari, Design, synthesis, in silico and biological evaluation of novel 2-(4-(4-substituted piperazin-1-yl)benzylidene)hydrazine carboxamides, Mol Divers 21(1) (2017) 163-174.

[8] G. De Simone, C.T. Supuran, Carbonic anhydrase IX: Biochemical and crystallographic characterization of a novel antitumor target, Biochimica et Biophysica Acta (BBA)-Proteins and Proteomics 1804(2) (2010) 404-409.

[9] D. Neri, C.T. Supuran, Interfering with pH regulation in tumours as a therapeutic strategy, Nature reviews Drug discovery 10(10) (2011) 767-777.

[10] J. Chiche, K. Ilc, J. Laferrière, E. Trottier, F. Dayan, N.M. Mazure, M.C. Brahimi-Horn, J. Pouysségur, Hypoxia-inducible carbonic anhydrase IX and XII promote tumor cell growth by counteracting acidosis through the regulation of the intracellular pH, Cancer research 69(1) (2009) 358-368.

[11] N.K. Tafreshi, M.C. Lloyd, M.M. Bui, R.J. Gillies, D.L. Morse, Carbonic anhydrase IX as an imaging and therapeutic target for tumors and metastases, Carbonic Anhydrase: Mechanism, Regulation, Links to Disease, and Industrial Applications, Springer2014, pp. 221-254.

[12] C. Potter, A.L. Harris, Hypoxia inducible carbonic anhydrase IX, marker of tumour: hypoxia, survival pathway and therapy target, Cell cycle 3(2) (2004) 159-162.

[13] S. Pastorekova, C.T. Supuran, Carbonic anhydrase IX: from biology to therapy, Hypoxia and Cancer, Springer2014, pp. 121-153.

[14] S. Rockwell, I.T. Dobrucki, E.Y. Kim, S.T. Marrison, V.T. Vu, Hypoxia and radiation therapy: past history, ongoing research, and future promise, Current molecular medicine 9(4) (2009) 442-458.

[15] S. Kumari, D. Idrees, C.B. Mishra, A. Prakash, Wahiduzzaman, F. Ahmad, M.I. Hassan, M. Tiwari, Design and synthesis of a novel class of carbonic anhydrase-IX inhibitor 1-(3-(phenyl/4-fluorophenyl)-7-imino-3H-[1,2,3]triazolo[4,5d]pyrimidin 6(7H)yl)urea, J Mol Graph Model 64 (2016) 101-9.

[16] M.M. Gottesman, Mechanisms of cancer drug resistance, Annu Rev Med 53 (2002) 615-27.

[17] M.O. Karataş, B. Alici, Ü. Çakir, E. Çetinkaya, D. Demir, A. Ergün, N. Gençer, O. Arslan, New coumarin derivatives as carbonic anhydrase inhibitors, Artificial cells, nanomedicine, and biotechnology 42(3) (2014) 192-198.

[18] M. Ferraroni, F. Carta, A. Scozzafava, C.T. Supuran, Thioxocoumarins show an alternative carbonic anhydrase inhibition mechanism compared to coumarins, Journal of medicinal chemistry 59(1) (2015) 462-473.

[19] A. Casini, J. Antel, F. Abbate, A. Scozzafava, S. David, H. Waldeck, S. Schäfer, C.T. Supuran, Carbonic anhydrase inhibitors: SAR and X-ray crystallographic study for the interaction of sugar sulfamates/sulfamides with isozymes I, II and IV, Bioorganic & medicinal chemistry letters 13(5) (2003) 841-845.

[20] C.T. Supuran, Carbonic anhydrase inhibitors, Bioorganic & medicinal chemistry letters 20(12) (2010) 3467-3474.

[21] A. Cecchi, A. Hulikova, J. Pastorek, S. Pastoreková, A. Scozzafava, J.-Y. Winum, J.-L. Montero, C.T. Supuran, Carbonic anhydrase inhibitors. Design of fluorescent sulfonamides as probes of tumor-associated carbonic anhydrase IX that inhibit isozyme IX-mediated acidification of hypoxic tumors, Journal of medicinal chemistry 48(15) (2005) 4834-4841.

[22] J. Pichake, P.S. Kharkar, M. Ceruso, C.T. Supuran, M.P. Toraskar, Carbonic anhydrase inhibitors: design, synthesis, and biological evaluation of novel sulfonyl semicarbazide derivatives, ACS medicinal chemistry letters 5(7) (2014) 793-796.

[23] C.T. Supuran, A. Scozzafava, A. Casini, Carbonic anhydrase inhibitors, Medicinal research reviews 23(2) (2003) 146-189.

[24] N. Korkmaz, O.A. Obaidi, M. Senturk, D. Astley, D. Ekinci, C.T. Supuran, Synthesis and biological activity of novel thiourea derivatives as carbonic anhydrase inhibitors, Journal of enzyme inhibition and medicinal chemistry 30(1) (2015) 75-80.

[25] O. Talaz, H. Çavdar, S. Durdagi, H. Azak, D. Ekinci, Synthesis of 1, 4-bis (indolin-1-ylmethyl) benzene derivatives and their structure–activity relationships for the interaction of human carbonic anhydrase isoforms I and II, Bioorganic & medicinal chemistry 21(6) (2013) 1477-1482.

[26] J. Pichake, P.S. Kharkar, M. Ceruso, C.T. Supuran, M.P. Toraskar, Carbonic anhydrase inhibitors: design, synthesis, and biological evaluation of novel sulfonyl semicarbazide derivatives, ACS medicinal chemistry letters 5(7) (2014) 793.

[27] A. Karioti, M. Ceruso, F. Carta, A.-R. Bilia, C.T. Supuran, New natural product carbonic anhydrase inhibitors incorporating phenol moieties, Bioorganic & medicinal chemistry 23(22) (2015) 7219-7225.

[28] S. Gemma, G. Kukreja, C. Fattorusso, M. Persico, M.P. Romano, M. Altarelli, L. Savini, G. Campiani, E. Fattorusso, N. Basilico, Synthesis of N1-arylidene-N2-quinolyl-and N2-acrydinylhydrazones as potent antimalarial agents active against CQ-resistant P. falciparum strains, Bioorganic & medicinal chemistry letters 16(20) (2006) 5384-5388.

[29] A. Inam, S.M. Siddiqui, T.S. Macedo, D.R.M. Moreira, A.C.L. Leite, M.B.P. Soares, A. Azam, Design, synthesis and biological evaluation of 3-[4-(7-chloro-quinolin-4-yl)-piperazin-1-yl]-propionic acid hydrazones as antiprotozoal agents, European journal of medicinal chemistry 75 (2014) 67-76.

[30] N. Terzioglu, A. Gürsoy, Synthesis and anticancer evaluation of some new hydrazone derivatives of 2, 6-dimethylimidazo [2, 1-b][1, 3, 4] thiadiazole-5-carbohydrazide, European journal of medicinal chemistry 38(7) (2003) 781-786.

[31] M.T. Cocco, C. Congiu, V. Lilliu, V. Onnis, Synthesis and in vitro antitumoral activity of new hydrazinopyrimidine-5-carbonitrile derivatives, Bioorganic & medicinal chemistry 14(2) (2006) 366-372.

[32] T. Nasr, S. Bondock, M. Youns, Anticancer activity of new coumarin substituted hydrazide–hydrazone derivatives, European journal of medicinal chemistry 76 (2014) 539-548.

[33] J. Easmon, G. Pürstinger, K.-S. Thies, G. Heinisch, J. Hofmann, Synthesis, structure− activity relationships, and antitumor studies of 2-benzoxazolyl hydrazones derived from alpha-(N)-acyl heteroaromatics, Journal of medicinal chemistry 49(21) (2006) 6343-6350.

[34] S. Ghiya, Y.C. Joshi, Synthesis and antimicrobial evaluation of hydrazones derived from 4-methylbenzenesulfonohydrazide in aqueous medium, Medicinal Chemistry Research 25(5) (2016) 970-976.

[35] G.L. Backes, D.M. Neumann, B.S. Jursic, Synthesis and antifungal activity of substituted salicylaldehyde hydrazones, hydrazides and sulfohydrazides, Bioorg Med Chem 22(17) (2014) 4629-36.

[36] E. Jameel, H. Naz, P. Khan, M. Tarique, J. Kumar, S. Mumtazuddin, S. Ahamad, A. Islam, F. Ahmad, N. Hoda, M.I. Hassan, Design, synthesis, and biological evaluation of pyrimidine derivatives as potential inhibitors of human calcium/calmodulin-dependent protein kinase IV, Chem Biol Drug Des 89(5) (2017) 741-754.

[37] G.M. Morris, R. Huey, W. Lindstrom, M.F. Sanner, R.K. Belew, D.S. Goodsell, A.J. Olson, AutoDock4 and AutoDockTools4: Automated docking with selective receptor flexibility, J Comput Chem 30(16) (2009) 2785-91.

[38] D.S. BIOVIA, Discovery Studio Modeling Environment, San Diego: Dassault Syste`mes (2013).

[39] A. Prakash, D. Idrees, M.A. Haque, A. Islam, F. Ahmad, M.I. Hassan, GdmCl-induced unfolding studies of human carbonic anhydrase IX: a combined spectroscopic and MD simulation approach, J Biomol Struct Dyn (2016) 1-12.

[40] Wahiduzzaman, M.A. Dar, M.A. Haque, D. Idrees, M.I. Hassan, A. Islam, F. Ahmad, Characterization of folding intermediates during urea-induced denaturation of human carbonic anhydrase II, Int J Biol Macromol 95 (2017) 881-887.

[41] H. Naz, P. Khan, M. Tarique, S. Rahman, A. Meena, S. Ahamad, S. Luqman, A. Islam, F. Ahmad, M.I. Hassan, Binding studies and biological evaluation of beta-carotene as a potential inhibitor of human calcium/calmodulin-dependent protein kinase IV, Int J Biol Macromol 96 (2016) 161-170.

[42] Y. Li, H. Wang, E. Oosterwijk, Y. Selman, J.C. Mira, T. Medrano, K.T. Shiverick, S.C. Frost, Antibody-specific detection of CAIX in breast and prostate cancers, Biochem Biophys Res Commun 386(3) (2009) 488-92.

[43] M. Zat'ovicova, K. Tarabkova, E. Svastova, A. Gibadulinova, V. Mucha, L. Jakubickova, Z. Biesova, M. Rafajova, M. Ortova Gut, S. Parkkila, A.K. Parkkila, A. Waheed, W.S. Sly, I. Horak, J. Pastorek, S. Pastorekova, Monoclonal antibodies generated in carbonic anhydrase IX-deficient mice recognize different domains of tumour-associated hypoxia-induced carbonic anhydrase IX, J Immunol Methods 282(1-2) (2003) 117-34.

[44] A.M. Rieger, K.L. Nelson, J.D. Konowalchuk, D.R. Barreda, Modified annexin V/propidium iodide apoptosis assay for accurate assessment of cell death, J Vis Exp (50) (2011).

[45] M.J. Cecchini, M. Amiri, F.A. Dick, Analysis of cell cycle position in mammalian cells, JoVE (Journal of Visualized Experiments) (59) (2012) e3491-e3491.

[46] H.H. Wong, N.R. Lemoine, Pancreatic cancer: molecular pathogenesis and new therapeutic targets, Nat Rev Gastroenterol Hepatol 6(7) (2009) 412-22.

[47] B.B. Hafeez, A. Mustafa, J.W. Fischer, A. Singh, W. Zhong, M.O. Shekhani, L. Meske, T. Havighurst, K. Kim, A.K. Verma, alpha-Mangostin: a dietary antioxidant derived from the pericarp of Garcinia mangostana L. inhibits pancreatic tumor growth in xenograft mouse model, Antioxid Redox Signal 21(5) (2014) 682-99.

[48] H. Naz, M. Tarique, P. Khan, S. Luqman, S. Ahamad, A. Islam, F. Ahmad, M.I. Hassan, Evidence of vanillin binding to CAMKIV explains the anti-cancer mechanism in human hepatic carcinoma and neuroblastoma cells, Mol Cell Biochem (2017).

[49] M.I. Hassan, V. Kumar, T.P. Singh, S. Yadav, Structural model of human PSA: a target for prostate cancer therapy, Chem Biol Drug Des 70(3) (2007) 261-7.

[50] M.I. Hassan, V. Kumar, R.K. Somvanshi, S. Dey, T.P. Singh, S. Yadav, Structure-guided design of peptidic ligand for human prostate specific antigen, J Pept Sci 13(12) (2007) 849-55.

[51] N. Hoda, H. Naz, E. Jameel, A. Shandilya, S. Dey, M.I. Hassan, F. Ahmad, B. Jayaram, Curcumin specifically binds to the human calcium-calmodulin-dependent protein kinase IV: fluorescence and molecular dynamics simulation studies, J Biomol Struct Dyn 34(3) (2016) 572-84.

[52] M.I. Hassan, Editorial. Recent Advances in the Structure-Based Drug Design and Discovery, Curr Top Med Chem 16(9) (2016) 899-900.

[53] F.I. Khan, M. Shahbaaz, K. Bisetty, A. Waheed, W.S. Sly, F. Ahmad, M.I. Hassan, Large scale analysis of the mutational landscape in beta-glucuronidase: A major player of mucopolysaccharidosis type VII, Gene 576(1 Pt 1) (2016) 36-44.

[54] F.I. Khan, D.Q. Wei, K.R. Gu, M.I. Hassan, S. Tabrez, Current updates on computer aided protein modeling and designing, Int J Biol Macromol 85 (2016) 48-62.

[55] P. Khan, A. Shandilya, B. Jayaram, A. Islam, F. Ahmad, M.I. Hassan, Effect of pH on the stability of hemochromatosis factor E: a combined spectroscopic and molecular dynamics simulation-based study, J Biomol Struct Dyn 35(7) (2017) 1582-1598.

[56] F. Naz, N. Sami, A. Islam, F. Ahmad, M.I. Hassan, Ubiquitin-associated domain of MARK4 provides stability at physiological pH, Int J Biol Macromol 93(Pt A) (2016) 1147-1154.

[57] F. Naz, M. Shahbaaz, S. Khan, K. Bisetty, A. Islam, F. Ahmad, M.I. Hassan, PKR-inhibitor binds efficiently with human microtubule affinity-regulating kinase 4, J Mol Graph Model 62 (2015) 245-52.

[58] M. Shahbaaz, K. Bisetty, F. Ahmad, M.I. Hassan, Current Advances in the Identification and Characterization of Putative Drug and Vaccine Targets in the Bacterial Genomes, Curr Top Med Chem 16(9) (2016) 1040-69.

[59] P.K. Thakur, I. Hassan, Discovering a potent small molecule inhibitor for gankyrin using de novo drug design approach, Int J Comput Biol Drug Des 4(4) (2011) 373-86.

[60] P.K. Thakur, J. Kumar, D. Ray, F. Anjum, M.I. Hassan, Search of potential inhibitor against New Delhi metallo-beta-lactamase 1 from a series of antibacterial natural compounds, J Nat Sci Biol Med 4(1) (2013) 51-6.

[61] S. Faes, A. Planche, E. Uldry, T. Santoro, C. Pythoud, J.-C. Stehle, J. Horlbeck, I. Letovanec, N. Riggi, D. Datta, Targeting carbonic anhydrase IX improves the anti-cancer efficacy of mTOR inhibitors, Oncotarget 7(24) (2016) 36666.

Figure Legends

Fig. 1: Structure of some known carbonic anhydrase inhibitors.

Fig. 2: Strategy for designing of carbonic anhydrase IX inhibitors.

Fig. 3: Molecular docking of synthesized compounds with CAIX: (A) 2D schematic diagram showing interactions of compound **1**, **2** and **3** to the CAIX. Residues involved in hydrogen bonding, charge or polar interactions, van der Waals interactions are represented in different color indicated in inset. **(B)** Surface view of CAIX complexed with compound **1, 2** and **3**.

Fig. 4: Interaction analysis of CAIX-inhibitor complex: (A) Cartoon model of CAIX complexed with all three synthesized compounds. Docked poses of **(B)** compound **1 (C)** compound **2** and **(D)** compound **3** with CAIX.

Fig. 5: Fluorescence binding studies of *p*-toluene sulfonylhydrazone derivatives with CAIX. (A) Fluorescence spectra of CAIX (5-8 µM) with increasing concentrations of each compound (0-100 µM). Excitation wavelength was fixed to 280 nm and emission was recorded in the range 300-400 nm. **(B)** Modified Stern-Volmer plot showing quenching of CAIX by each compound used to calculate binding affinity (Ka).

Fig. 6: ITC measurement showing titration of p-toluene sulfonylhydrazone analogue with CAIX. (Top) Raw data plot of heat produced against time for the titration of 800-1200 µM **1**, **2** and **3** into 16-20 µM CAIX. (Bottom) Corresponding binding isotherm obtained after integration of peak area and normalization to yield a plot of molar enthalpy change against inhibitor-CAIX ratio. The one-site fit curve is displayed as a thin red color line.

Fig. 7: Cell viability assay. (A) Effect of CAIX inhibitors on the viability of human cancer cells (HeLa) and human normal cell (HEK-293) lines: Cells were treated with

increasing concentrations of each compound (0-100 μM) for 48 h. In case of hypoxia-induced cells, we first exposed the cells to hypoxic conditions for 24 h, and then treatment is given. Cell viabilities to that of the control were shown here. Each data point shown is the mean ± SD from n=3. **(B)** Effect of CAIX inhibitors on the viability of human cancer cells (HeLa) and human normal cell (HEK-293) lines: Cells were treated with increasing concentrations of each compound (0-100 μM) for 48 h. Cell viabilities to that of the control were shown here. Each data point shown is the mean ± SD from n=3

Fig. 8: Cell apoptosis studies. (A) Annexin-V staining of HT-29 and HeLa cells; cells were treated with IC_{50} concentration of each inhibitor for 24 h and subsequently stained with FITC-Annexin-V/7-AAD-staining. Apoptosis was quantified by flow cytometry. Representative flow images showing FITC-Annexin-V/7-AAD labeled cells, which directly corresponds to the percentage of apoptotic cells. **(B)** Representative images of HeLa cells stained with DAPI after the treatment of each compound, apoptotic nuclei were marked by red color arrow heads.

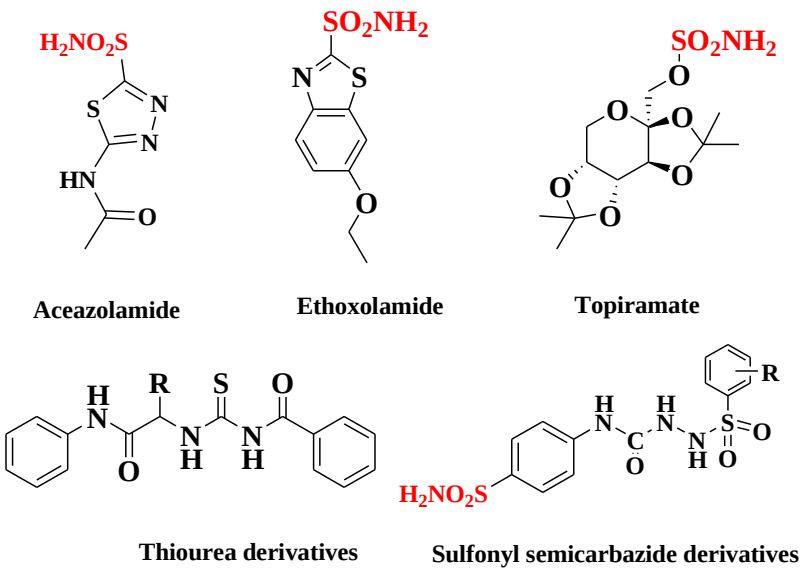

Figure 1

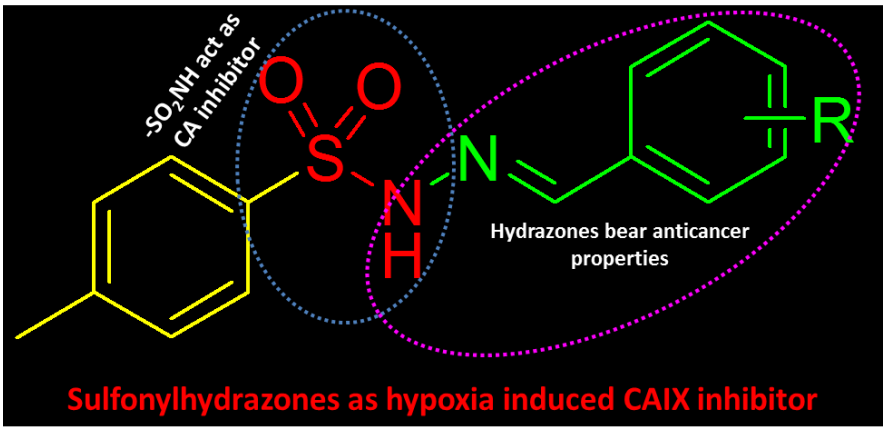

Figure 2

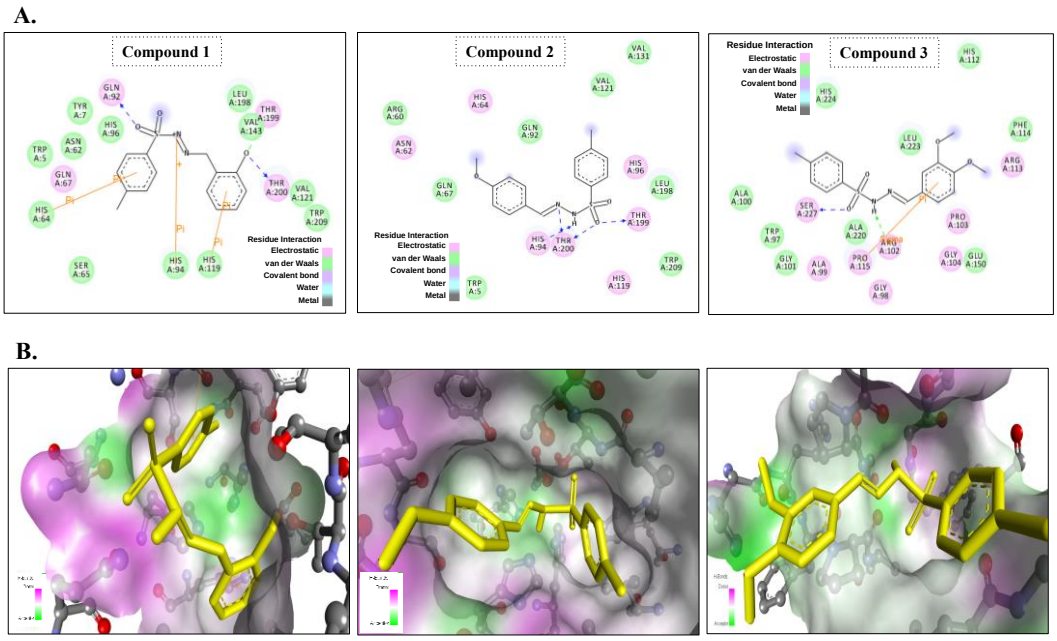

Figure 3

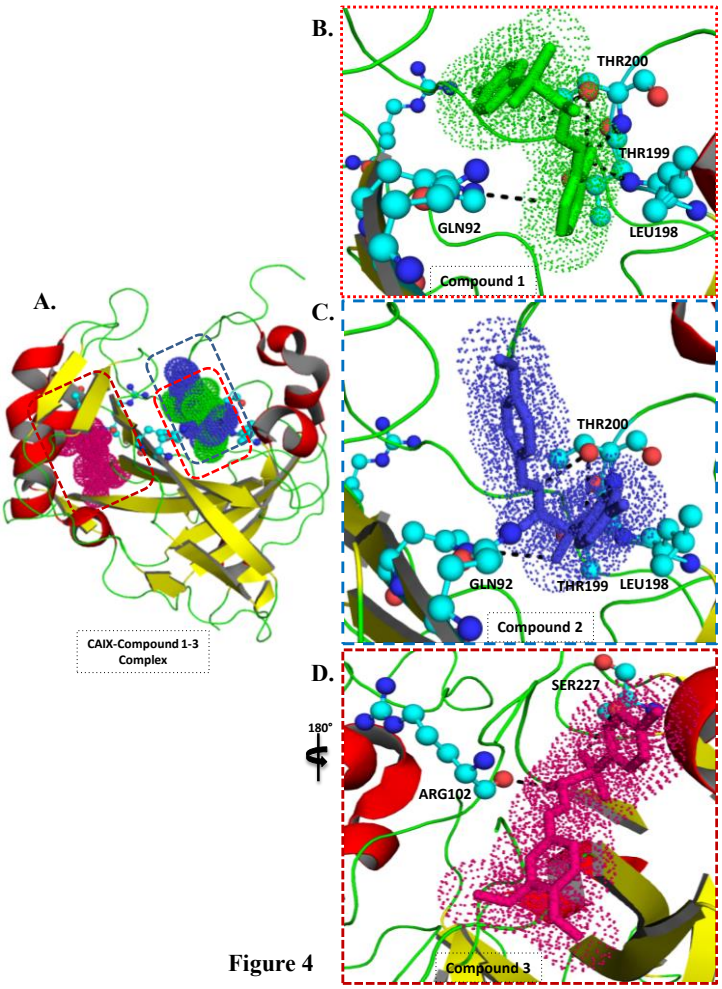

Figure 4

A.

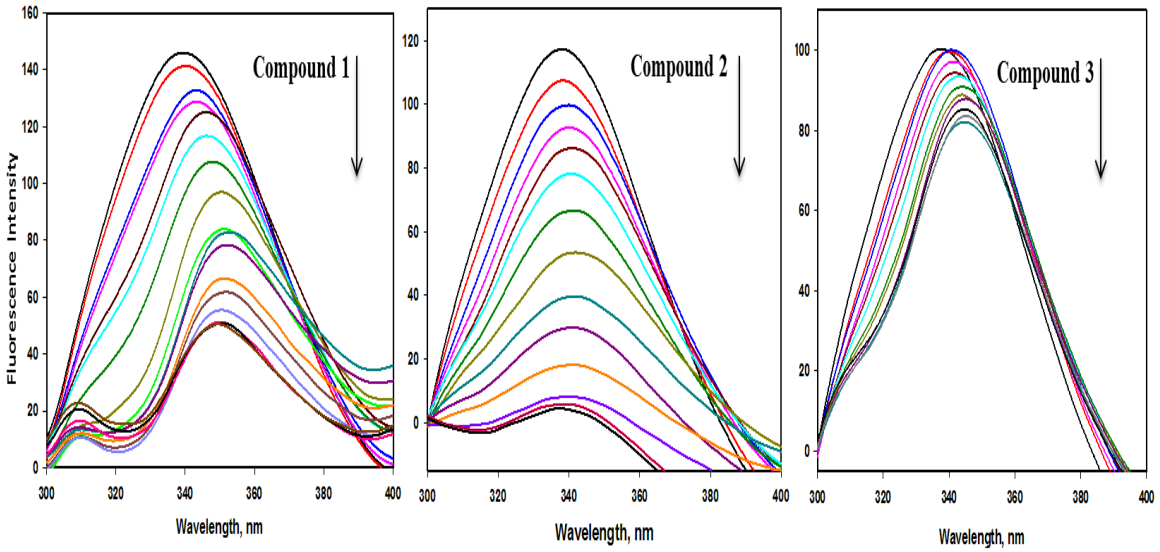

B.

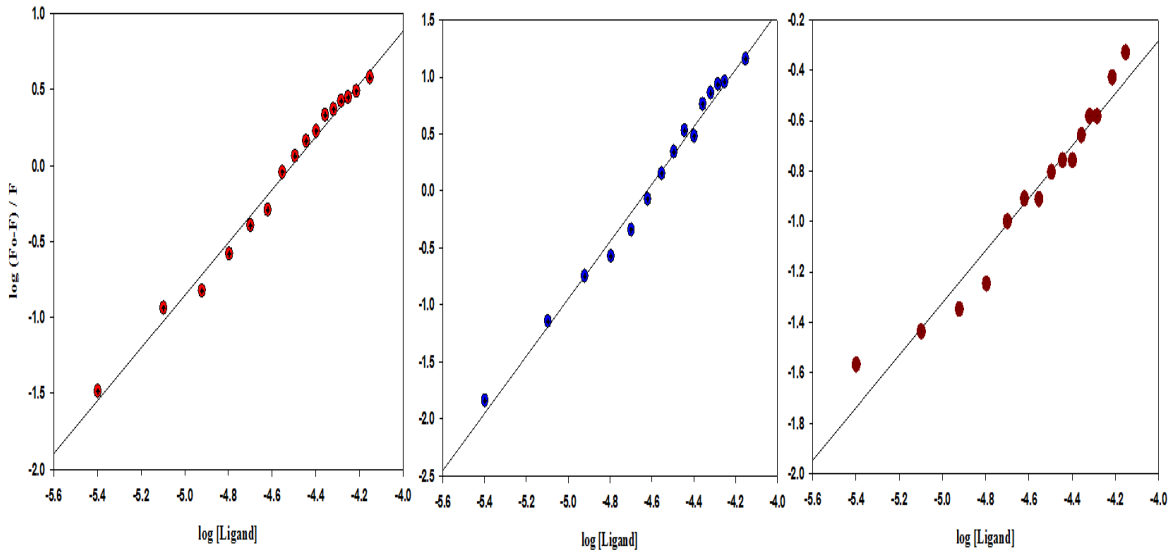

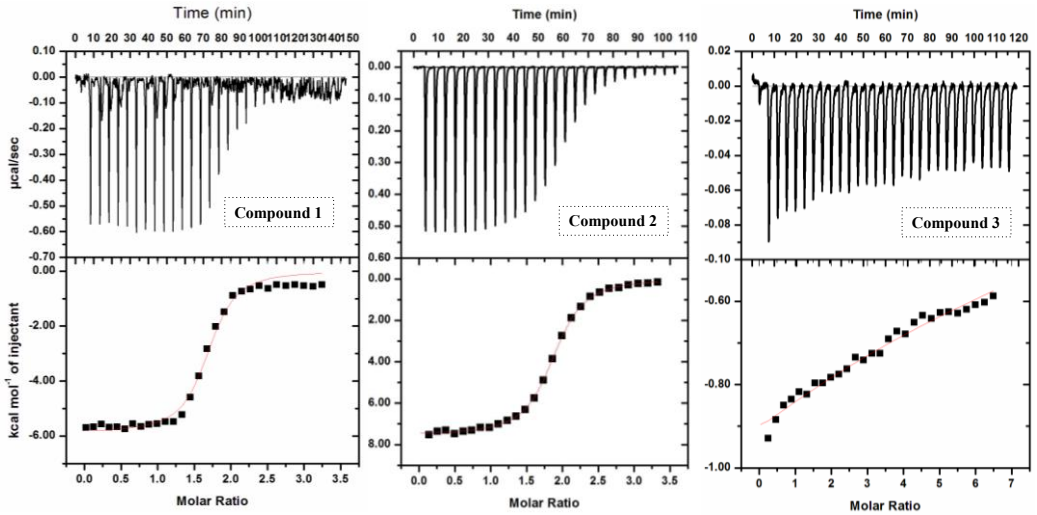

Figure 6

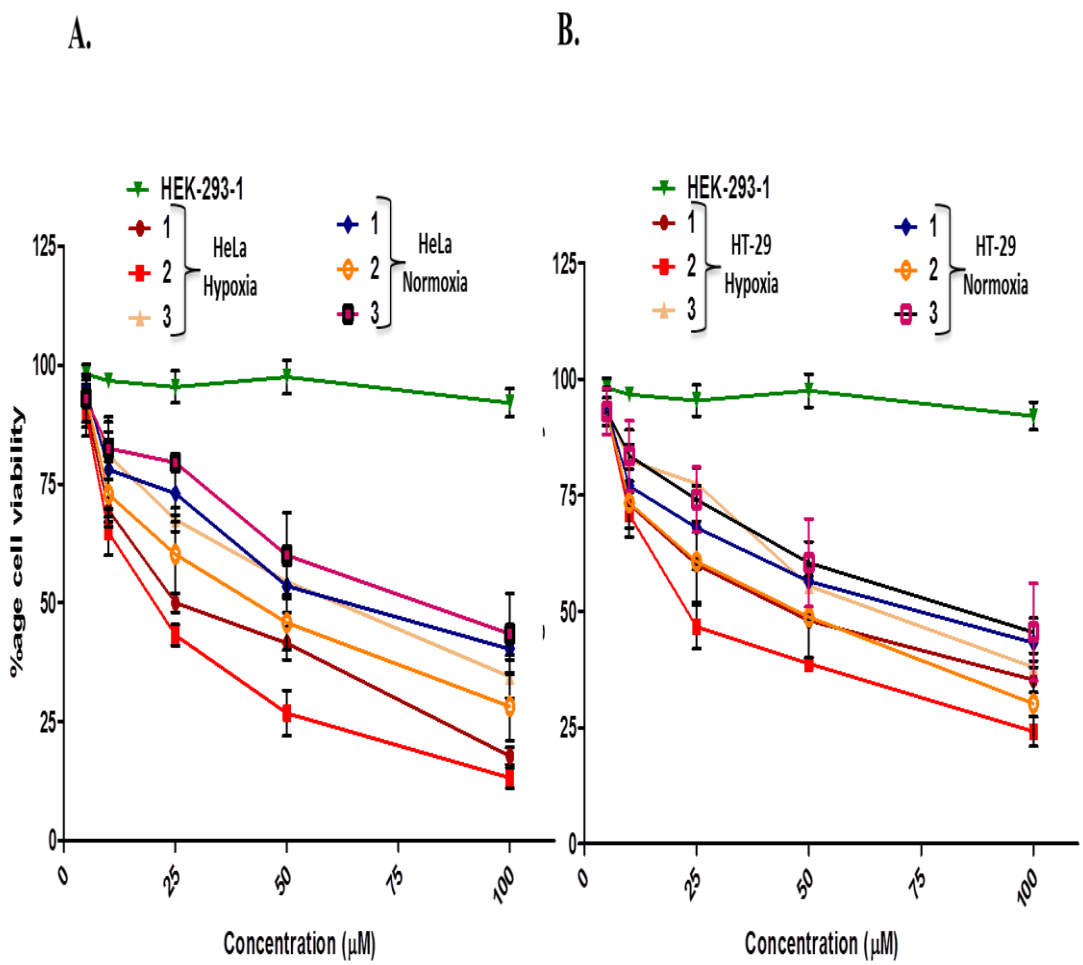

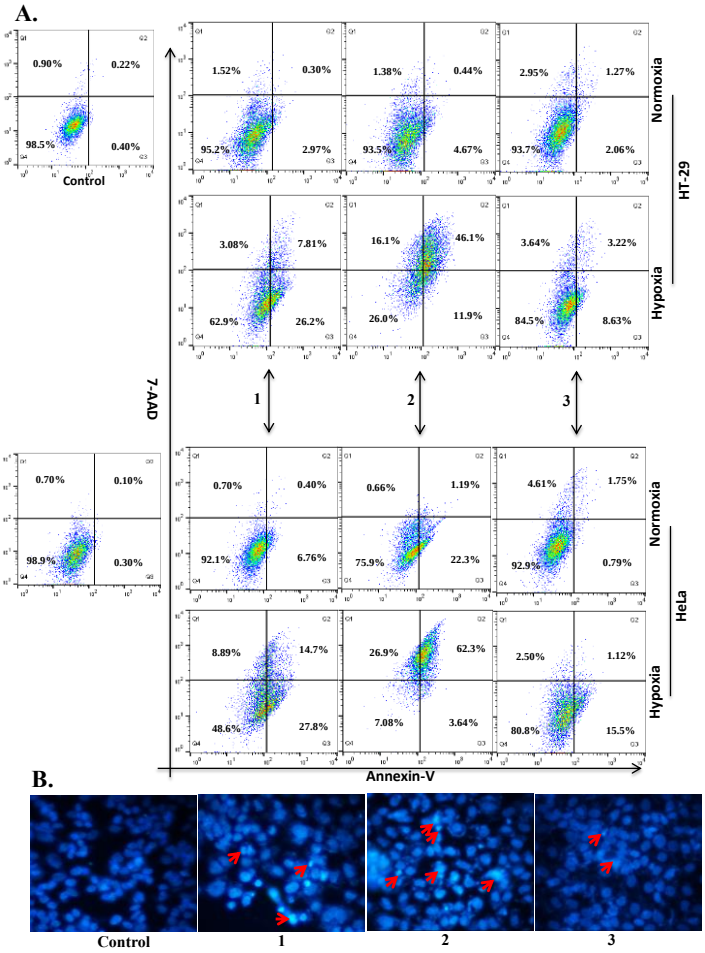

Figure 8

Table1: Parameters obtained from molecular docking studies.

Compound	Binding Energy (kcal/mol)	No. of hydrogen bonds	Hydrogen bond forming residues	Distances (Å)	Other interacting residues
1	-7.9	4	Gln92 Leu198 Thr199 Thr200	3.0 3.1 3.0 2.7	Trp5, Tyr7, Asn62, His64, Ser65, Gln67, Val121, Val143, His94, His96, His119, Trp209
2	-8.1	6	His94 Thr199 Thr199 Thr200 Thr200 Thr200	3.3 2.8 3.0 3.0 3.0 2.9	Trp5, Arg60, Asn62, His64, Gln67, Gln92, His96, His119, Val121, Val131, Leu198, Trp209
3	-7.6	2	Arg102 Ser227	2.2 3.0	Trp97, Gly98, Ala99, Ala100, Gly101, Pro103, Gly104, His112, Arg113, Phe114, Pro115, Glu150, Ala220, Leu223, His224

Table 2: Thermodynamic parameters and functional activity concentrations obtained from ITC, enzyme inhibition and MTT assay.

Compound	§K_a, (M^{-1})	ΔH, cal/mol	§K_D, (μM)	¶K_D	¥IC_{50}, (nM), CAIX	¥IC_{50}, (μM), CAII	ψIC_{50}, (μM), HeLa	ψIC_{50}, (μM), HT-29
1	$1.28\times 10^6 \pm 1.38\times 10^5$	$-5.94\times 10^2 \pm 6.77$	0.781	14.49 nM	78	99	24.12 ± 2.13	37.20± 2.00
2	$3.60\times 10^6 \pm 1.03\times 10^5$	$-7.544\times 10^3 \pm 19.26$	0.277	2.38 nM	56	90	18.02± 1.12	28.03±1.15
3	$2.4\times 10^3 \pm 1.0\times 10^2$	$-3.52\times 10^2 \pm 1.26\times 10^3$	414	135.13 μM	1056	160	62.14± 2.5	75.50±2.20

§=From ITC, ¶= from fluorescence, ¥= from enzyme inhibition, ψ= from MTT for hypoxic cells